AD-A078 797 NORTHEASTERN UNIV BOSTON MASS ELECTRONICS RESEARCH LAB F/G 14/2
AN RF OSCILLATOR FOR ROCKET-BORNE AND BALLOON-BORNE QUADRUPOLE --ETC(U)
SEP 79 T A PALASEK F19628-78-C-0218
UNCLASSIFIED SCIENTIFIC-2 AFGL-TR-79-0226 NL

| OF |
AD A078 797

END
DATE FILMED
1-80
DDC

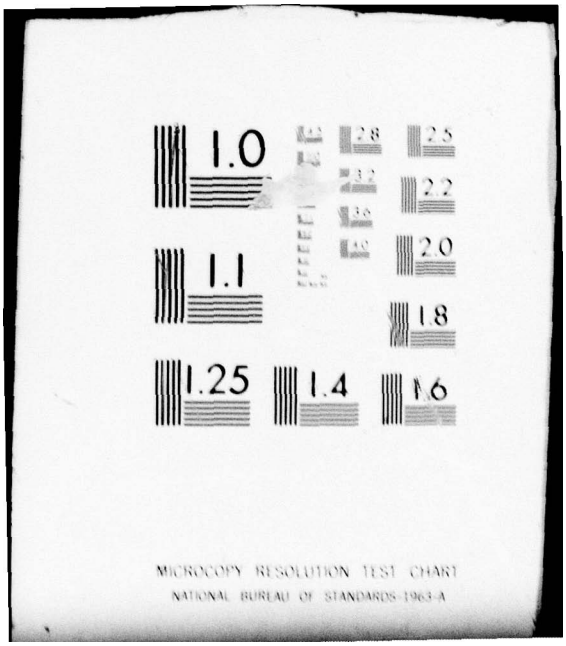
1.0
1.1
1.25
1.4
1.6
2.8
2.5
3.2
2.2
3.6
2.0
4.0
1.8
MICROCOPY RESOLUTION TEST CHART
NATIONAL BUREAU OF STANDARDS-1963-A

AFGL-TR-79- 0226

12

AN RF OSCILLATOR FOR ROCKET-BORNE AND BALLOON-BORNE QUADRUPOLE MASS SPECTROMETERS

Thomas A. Palasek

Northeastern University
Electronics Research Laboratory
Boston, Massachusetts 02115

SCIENTIFIC REPORT NO. 2

10 September 1979

Approved for public release; distribution unlimited

Prepared for

Air Force Geophusics Laboratory
Air Force Systems Command
United States Air Force
Hanscom AFB, Massachusetts 01731

(14) SCIENTIFIC-2

MIL-STD-847A
31 January 1973

Unclassified
SECURITY CLASSIFICATION OF THIS PAGE (When Data Entered)

(19) REPORT DOCUMENTATION PAGE

READ INSTRUCTIONS BEFORE COMPLETING FORM

(18) 1. REPORT NUMBER AFGL-TR-79-0226	2. GOVT ACCESSION NO. / 3. RECIPIENT'S CATALOG NUMBER /
(6) 4. TITLE (and Subtitle) AN RF OSCILLATOR FOR ROCKET-BORNE AND BALLOON-BORNE QUADRUPOLE MASS SPECTROMETERS	5. TYPE OF REPORT & PERIOD COVERED (9) Scientific Report No. 2 Interim 6. PERFORMING ORG. REPORT NUMBER
7. AUTHOR(s) (10) Thomas A. Palasek	8. CONTRACT OR GRANT NUMBER(s) F1928-78-C-0218
9. PERFORMING ORGANIZATION NAME AND ADDRESS Northeastern University Electronics Research Boston, MA 02115	10. PROGRAM ELEMENT, PROJECT, TASK AREA & WORK UNIT NUMBERS 61102F (16) 2310G3AM (17) G3
11. CONTROLLING OFFICE NAME AND ADDRESS Air Force Geophysical Laboratory (11) Hanscom AFB, Massachusetts 01731 Monitor/ Alan D. Bailey LKD	12. REPORT DATE 10 September 1979 13. NUMBER OF PAGES 45 (12) 46
14. MONITORING AGENCY NAME & ADDRESS(if different from Controlling Office)	15. SECURITY CLASS. (of this report) Unclassified 15a. DECLASSIFICATION DOWNGRADING SCHEDULE

16. DISTRIBUTION STATEMENT (of this Report)

Approved for public release; distribution unlimited

17. DISTRIBUTION STATEMENT (of the abstract entered in Block 20, if different from Report)

(15) F19628-78-C-0218, F19628-76-C-0256

18. SUPPLEMENTARY NOTES

19. KEY WORDS (Continue on reverse side if necessary and identify by block number)

Mass Spectrometer	Sweep Voltage
Quadrupole	Linearity
RF oscillator	Temperature Stabilization
RF Transformer	Radiofrequency

20. ABSTRACT (Continue on reverse side if necessary and identify by block number)

This thesis deals with the development of an (RF) Oscillator used in rocket-borne and balloon-borne quadrupole mass spectrometers. A new toroidal-shaped RF transformer has been developed along wi with new control circuitry for the modified Hartly oscillator that is used. Solutions to the problems of temperature stabilization and linearity are also discussed. Also included in this thesis is a review of quadrupole mass filter theory.

DD FORM 1 JAN 73 1473 EDITION OF 1 NOV 65 IS OBSOLETE

Unclassified
SECURITY CLASSIFICATION OF THIS PAGE (When Data Entered)

127 500 JCB

ACKNOWLEDGMENTS

I would like to thank my thesis advisor, Professor J. S. Rochefort, for his time and helpful criticism in writing this thesis, the work for which was done on AFGL Contract Number F19628-76-C-0256 and F19628-76-C-0218. I would also like to thank Mr. Raimundas Sukys and my fellow employees for their helpful suggestions. Finally, I wish to express my appreciation to Ms. Karen Dubé for doing such an excellent job of typing this thesis.

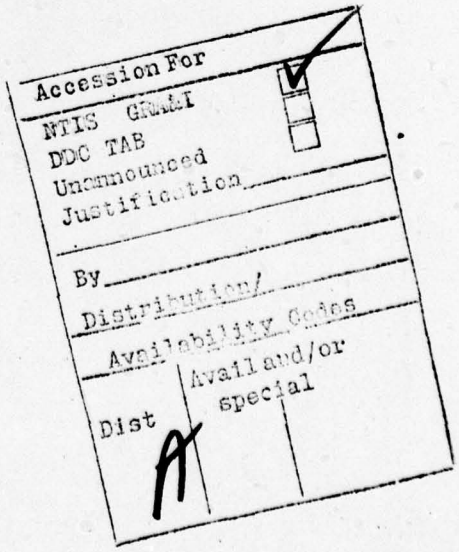

TABLE OF CONTENTS

Acknowledgments	iii
Table of Contents	v
List of Illustrations	vi
I. Introduction	1
II. Quadrupole Mass Filter-Theory of Operation	5
III. RF Oscillator	9
A. System Description	9
B. RF Oscillator Control Circuit Parameters	13
IV. RF Transformer	17
A. Empirical Determination of Transformer Size	17
B. Temperature Stabilization of RF Transformer	20
V. Peak Detector	24
A. Temperature Stabilization of the Peak Detector	24
B. Linearity of Peak Detector	24
VI. RF Oscillator Protection Circuit	33
References	38
Related Contracts	39
Personnel	40

List of Illustrations

Figure No.	Title	Page No.
1.	Quadrupole Mass Filter	3
2.	Block Diagram of RF Oscillator and Control Circuits	3
3.	Quadrupole Stability Diagram	7
4.	RF Transformer	10
5.	Previous RF Oscillator	12
6.	RF Oscillator	14
7.	Core Height VS Frequency	19
8.	Core Size VS Temperature	21
9.	Core Size VS Temperature	22
10.	Core Size VS Temperature	23
11.	Sweep Input VS RF Output for Uncompensated Peak Detector	31
12.	Sweep Input VS RF Output for Compensated Peak Detector	32

I. INTRODUCTION

Under Air Force contracts F19629-76-C-0256 and F19628-76-C-0218 four cluster ion mass spectrometers have been developed. These new instruments are very different than predecessors both in construction and operation.

Previous instruments were capable of detecting and measuring atomic mass units (amu) from 1 to almost 140. However, these new mass spectrometers are required to reach amu's of up to 255 in both the positive ion and negative ion modes. Since the frequency of the AC voltage applied to the mass filter was specified to be 2.3 MHz, a peak RF voltage of 725 volts is required to detect mass number 255.

Aside from this expanded amu range, a quadrupole mass filter with "delayed d-c field" constuction was adopted by the Aeronomy Division of the Air Force Geophysics Laboratory. This filter consists of two sets of quadrupole rods. One is used as a high mass pre-filter, the other is used as the main mass filter. Since these rods are longer than the ones used in previous instruments, the quadrupole capacitance has increased from 22pF to 81pF. Figure 1 represents this new quadrupole mass filter along with its appropriate control voltages.

In order to meet these voltage, frequency and load requirements; a new RF oscillator transformer with appropriate control circuitry had to be developed. The new transformer, which was proposed by Mr. Raimundas Sukys of Northeastern University, consists of two

torroidal acrylic cores, each containing a secondary winding; stacked on top of one another. The primary and feedback windings are then wound around both cores.

This new transformer is excellent for this application because of its small size and the torroidal shape of the cores tends to confine the magnetic field, and unlike previous instruments, it is less sensitive to its surroundings. This makes the adjustment of the oscillator and the calibration of the instrument easier.

However, there are many problems with the transformer and its control circuits. One of the major problems of the transformer is that its frequency and amplitude are sensitive to temperature changes and self heating effects. Another problem is that since the existing equations found in engineering handbooks for the inductance of torroidal cores didn't correlate with the data taken, empirical determination of the core size was necessary.

Figure 2 is a block diagram of the RF oscillator along with its control circuits. As can be seen from the diagram, a peak detector is incorporated into the feedback loop. It consists of a capasitor divider and integrator. Like the transformer, it too has instability problems, such as its sensitivity to temperature changes. Also, because of the limitations of the peak detector, it is not possible to obtain RF voltages low enough to select the first few amu's.

The oscillator may also enter a "lock-up" mode of operation. During this time excessive current will be drawn and control of the oscillator is lost. This will cause the power transistors of the oscillator to exceed their power rating, thus destroying these devices. Also,

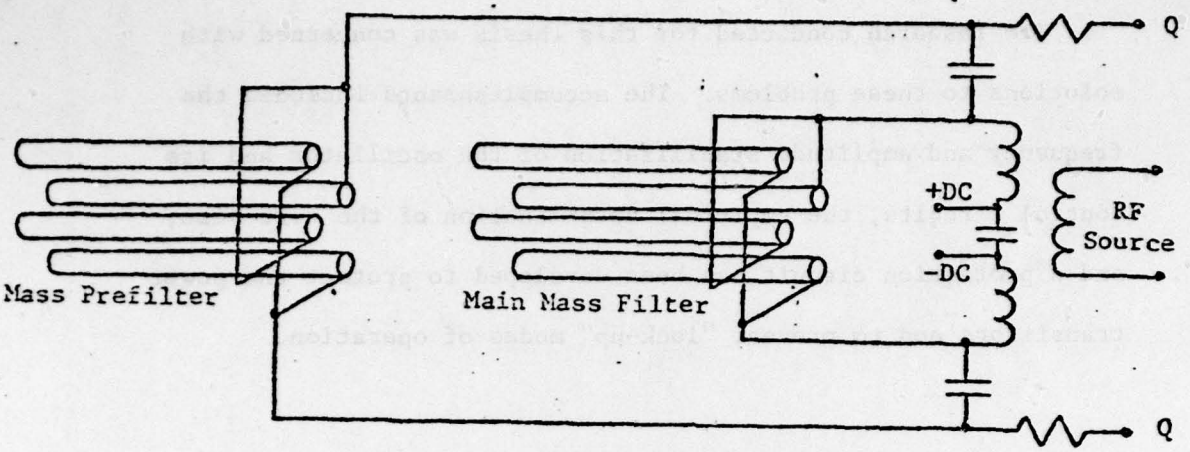

FIGURE 1. Quadrupole Mass Filter

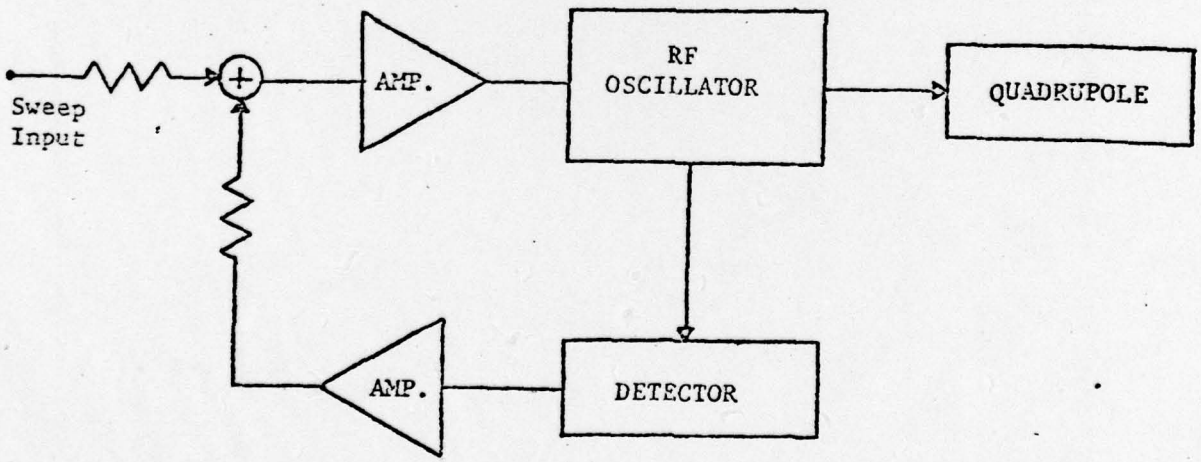

FIGURE 2. Block Diagram of RF Oscillator and Control Circuits

when it enters this "lock-up" mode, it usually oscillates at some high harmonic frequency.

The research conducted for this thesis was concerned with solutions to these problems. The accomplishments included the frequency and amplitude stabilization of the oscillator and its control circuits, the empirical determination of the core size; and a protection circuit has been developed to protect the power transistors and to prevent "lock-up" modes of operation.

II. QUADRUPOLE MASS FILTER-THEORY OF OPERATION

The basic mass analyzer used for lower ionospheric measurements is the quadrupole mass filter. The quadrupole mass filter consists of four circular rods with opposite rods electrocally connected together. The voltage applied between these rods has a radio frequency component V cos ωt and dc component U. The potential difference between the two sets of rods is thus U+V cos ωt.

When a positive ion is injected into the quadrupole region it oscillates between the rods of the mass filter. At a specific radio frequency this ion of given mass will undergo stable oscillation between the rods. Other ions of higher or lower masses will oscillate with increasing amplitude until they are absorbed by the rods. Within the quadrupole field there is no force in the longitudinal direction so that an ion under stable oscillating conditions will continue at its initial velocity until it reaches the collector target.

The equations [1,5] of motion for a charged positive ion within the region between the rods are:

$$m\ddot{x} + \frac{2e\ (U + V\cos\omega t)x}{r_o^2} = 0 \qquad (1)$$

$$m\ddot{y} - \frac{2e(U + V\cos\omega t)y}{r_o^2} = 0 \qquad (2)$$

$$m\ddot{z} = 0 \qquad (3)$$

Where:

r_o is 1/2 the spacing between rods of a pair

x and y are coordinates normal to the rod-pair axis

z is the coordinate along the rod-group axis

e is the charge on an electron

ω is the radian frequency of the RF component

t is the time

These Mathieu differential equations can be solved in terms of ion mass m, U and V cos ωt. The conditions for stable solutions may be seen with the aid of a stability diagram (Fig. 3) [2,5] in which the bounds between all useful stable solutions and unstable solutions are plotted in terms of the transformations.

$$a = \frac{8eU}{mr_o^2\omega^2} \qquad (4)$$

$$q = \frac{4eV}{mr_o^2\omega^2} \qquad (5)$$

If U and V are held constant, then from (4) and (5), the ratio of a to q will be constant and straight lines such as 1 and 2 in figure 1 will result. Under normal operating conditions the ratio U/V is chosen such as to intersect the top of the stability region and to abtain a high resolution. By choosing to operate the mass filter as in Line 2 in Figure 3, the quadrupole becomes a band-pass mass filter and all ions lying between m_1 and m_2 are then given by:

$$m_1 = \frac{4eV}{q_2 r_o^2 \omega^2} \qquad (6)$$

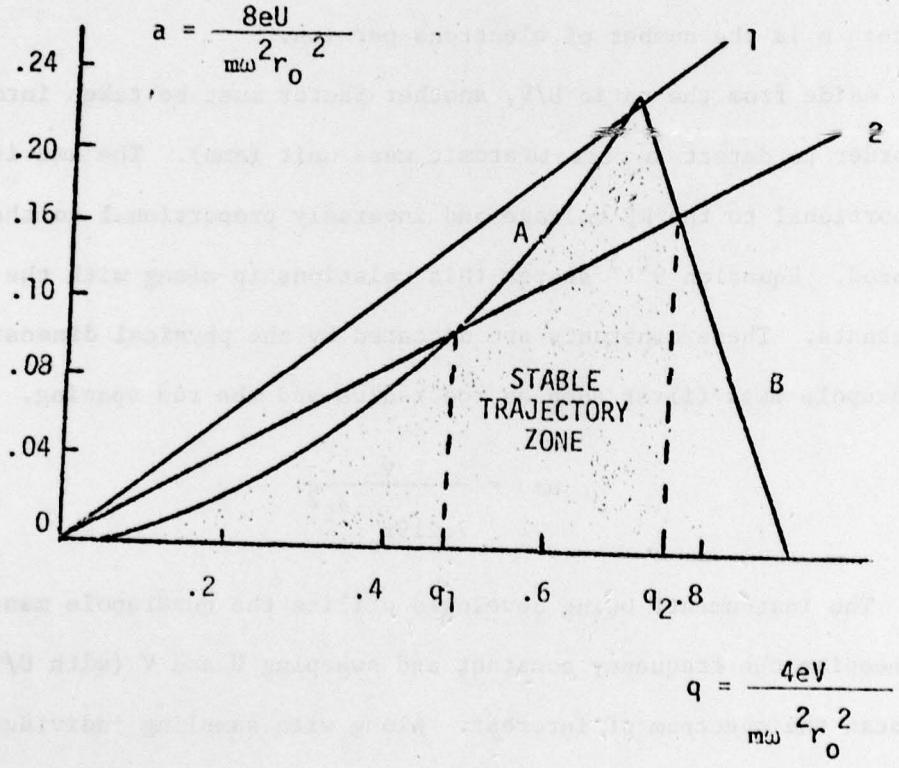

Figure 3. QUADRUPOLE STABILITY DIAGRAM

$$m_2 = \frac{4eV}{q_1 r_o^2 \omega^2} \qquad (7)$$

Thus the ratio U/V determines the filter pass band Δm and therefore the resolution $m/\Delta m$. Another useful feature of the quadrupole mass filter is the high-pass mode of operation. In this mode U=0 and the quadrupole will focus all ions for which the mass to charge ratio

$$\frac{m}{n} \geq \frac{4.4eV}{r_o^2 \omega^2} \qquad (8)$$

Where: n is the number of electrons per ion.

Aside from the ratio U/V, another factor must be taken into account in order to detect a certain atomic mass unit (amu). The amu is directly proportional to the RF voltage and inversely proportional to the frequency squared. Equation 9[1,5] states this relationship along with the appropriate constants. These constants are dictated by the physical dimensions of the quadrupole mass filter such as rod radius and the rod spacing.

$$\text{amu} = \frac{V}{7.219 r_o^2 f^2} \qquad (9)$$

The instruments being developed utilize the quadrupole mass filter by keeping the frequency constant and sweeping U and V (with U/V constant) to scan the spectrum of interest. Along with sampling individual amu's, the instruments will also utilize the high-pass mode (total ions) of operation.

III. RF OSCILLATOR

A. System Description

The basic oscillator is the same type that has been used in previous instruments. It is a tuned-secondary Hartley oscillator where the frequency of oscillation is determined by the induction of the output winding of the transformer and the quadrupole capacitance. Both the AC and DC components of the voltage that is applied to the quadrupole rods, are supplied from the oscillator. The ac component is generated by the oscillator and its amplitude is controlled by the feedback loop shown in Figure 2. The dc voltage is obtained from a sweep amplifier and is supplied to the oscillator transformer through an LC filter. This filter is necessary in order to prevent the RF voltage from feeding back into the sweep amplifier.

Although the basic oscillator is the same, the transformer is quite different. The transformers used in previous instruments were modified soleuoids in shape and were quite large as compared to the new toroidal shaped cores. These transformers and their and their associated control circuits were quite sensitive to the enviroment and had to be shielded before calibration of the instrument could be undertaken. This shielding made the adjustment of the oscillator rather difficult.

The new transformer consists of two toroidal acrylic cores stacked on top of one another. Figure 4 represents the manner in which these cores were wound. Each core contains a secondary winding of 155 turns of number 24 heavy armored polythermalaze wire. The cores are then insulated with strips of maylar. This insulation is necessary in

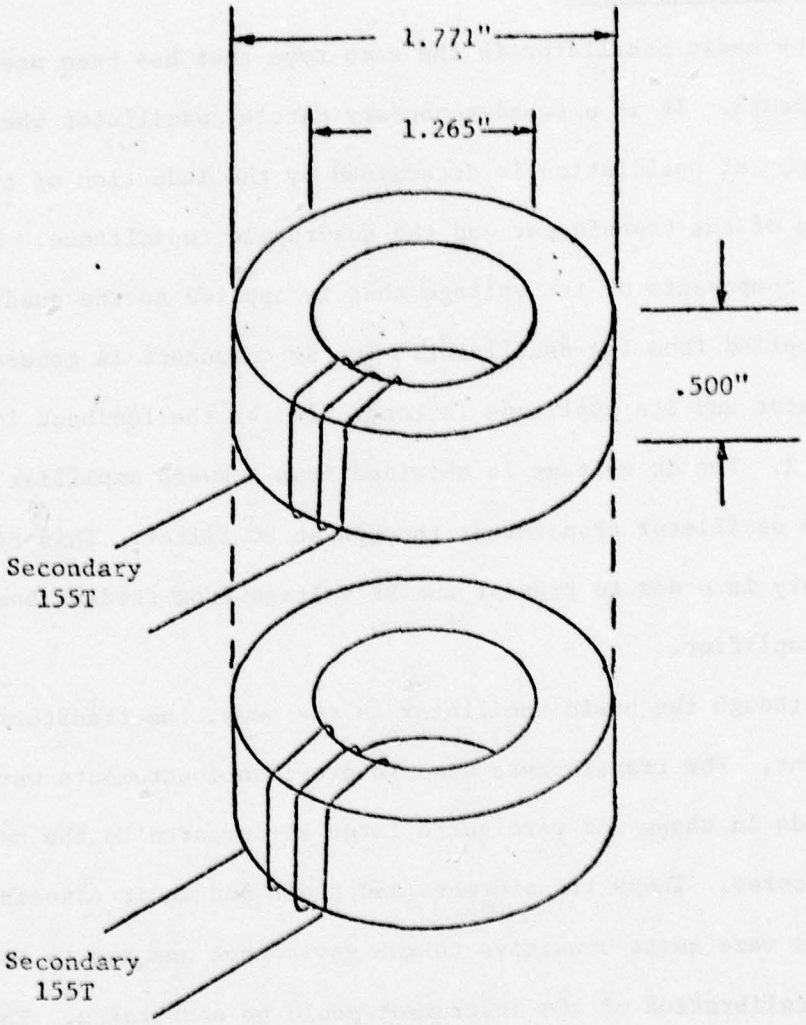

Note: Dimensions of cores are before baking.

FIGURE 4. RF TRANSFORMER

order to prevent high voltage arcs between the two cores. After the cores have been insulated, they are stacked on top of one another; and the primary windings of four turns and the feed back windings of two turns, both of number 22 heavy armored polythermalaze wire, are wound. For the convience of construction the primary and the feedback windings were displaced from each other by approximately 90° along the circumference of the core. Other winding distributions were tested without producing significant difference in the operation of the oscillator. Because the toroidal shape of the cores tends to confine the magnetic field and the fact that the transformer is totally enclosed within the oscillator housing, it is less sensitive to the enviroment. The empirical determination of the core size and the temperature stabilization of the transformer are discussed in Chapter 3.

Also, the method of controlling the amplitude of the RF voltage is quite different. In previous oscillators a separate winding of one turn was used to derive a feedback signal whose amplitude was proportional to the RF voltage (see Figure 5). [3] Since a separate winding was used, the induced voltage in this winding had a high harmonic content caused by switching transients in the primary circuit. This adversely effected the linearity of the RF voltage with respect to the sweep input voltage, causing the ratio of U/V to vary through the spectrum of interest.

From Figure 5 we see the feedback signal is divided by a resistor divider and applied to one of the imputs of the -710 comparator. The other input signal is obtained by feeding back the output of the comparator. This forms a peak detector. The output of the peak detector is then applied through a buffer amplifier to the inverting input of the -741 operational amplifier where it is summed with the sweep input voltage. This voltage will then drive the oscillator

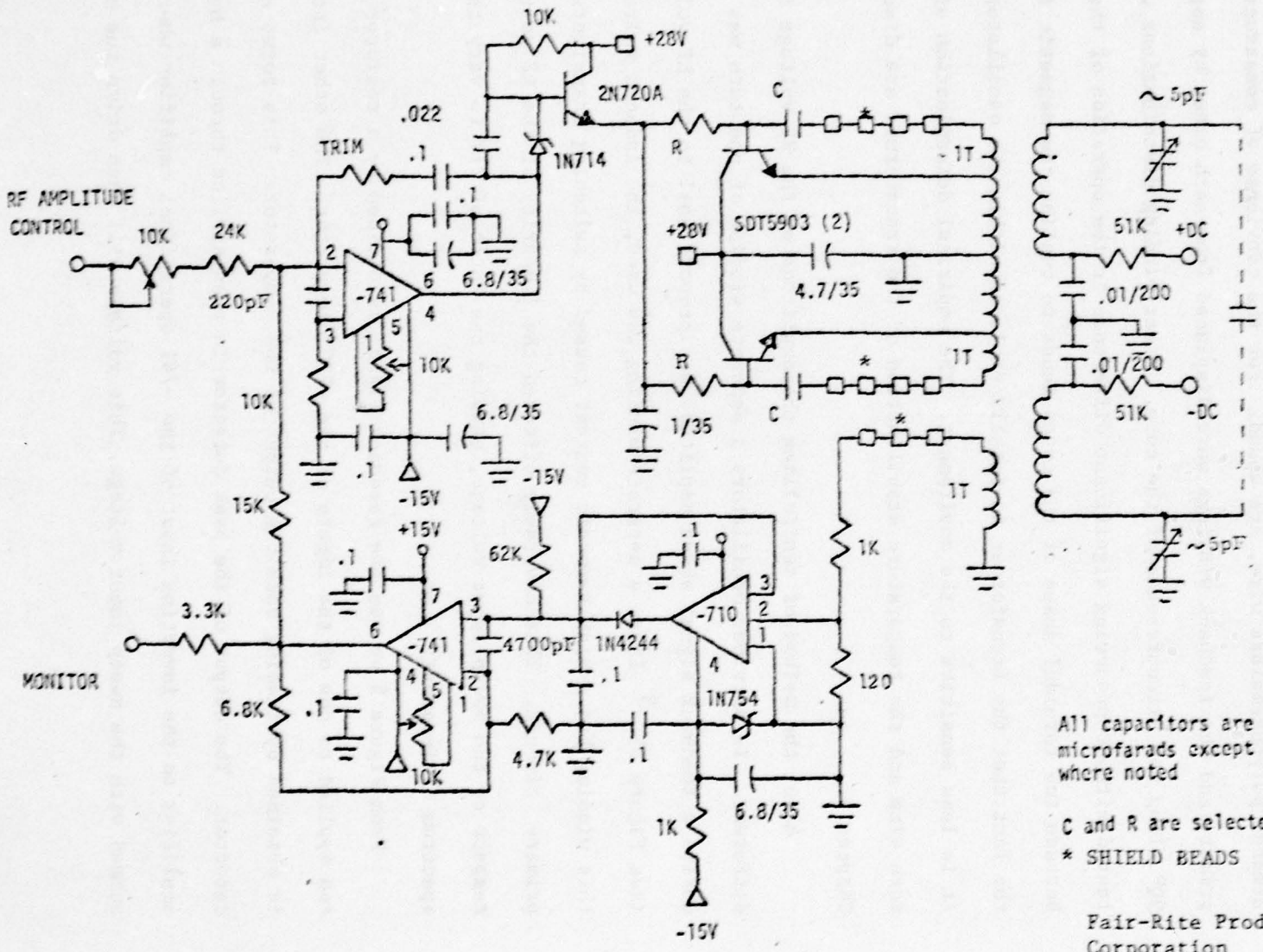

Figure 5. PREVIOUS RF OSCILLATOR

through the 2N270A transistor. The adjustment of the ratio U/V was accomplished through the use of the two offset potentiometers on the -741 op-amps.

The new oscillator with its control circuitry is shown in Figure 6. Since the mass filter must detect amu's of up to 255, the linearity of the RF oscillator is very important, especially at the higher mass numbers. In order to improve the linearity of the oscillator, the feedback signal is derived directly from the secondary winding of the transformer. The secondary is part of the tank circuit so the harmonic content in the RF voltage will be much less than the the separate feedback winding.

B. RF Oscillator Control Circuit Parameters

The control circuits for the RF oscillator are shown in Figure 6. The feedback loop consists of a peak detector, integrator and a summing amplifier. The CA 3140BT BiMos operational amplifier was selected for its low input offset voltage of 0.8mV and its low input offset current of 0.5pA at 25°C. Since these specifications are better that for the -741 operational amplifier, the variation of output voltage due to temperature variations are lower. This improves the linearity of the RF voltage with respect to the sweep input voltage.

The peak RF voltage (Vp) which is fedback from the oscillator transformer is divided by the capacitor devider consisting of capacitors C_1, C_2, C_3 and C_4. The divider will produce a voltage across C_4 equivalent to Vp/25. Since this voltage must be kept constant with respent to temperature variations, high reliability corning CYR glass capacitors were selected. These capacitors have a temperature coefficient of

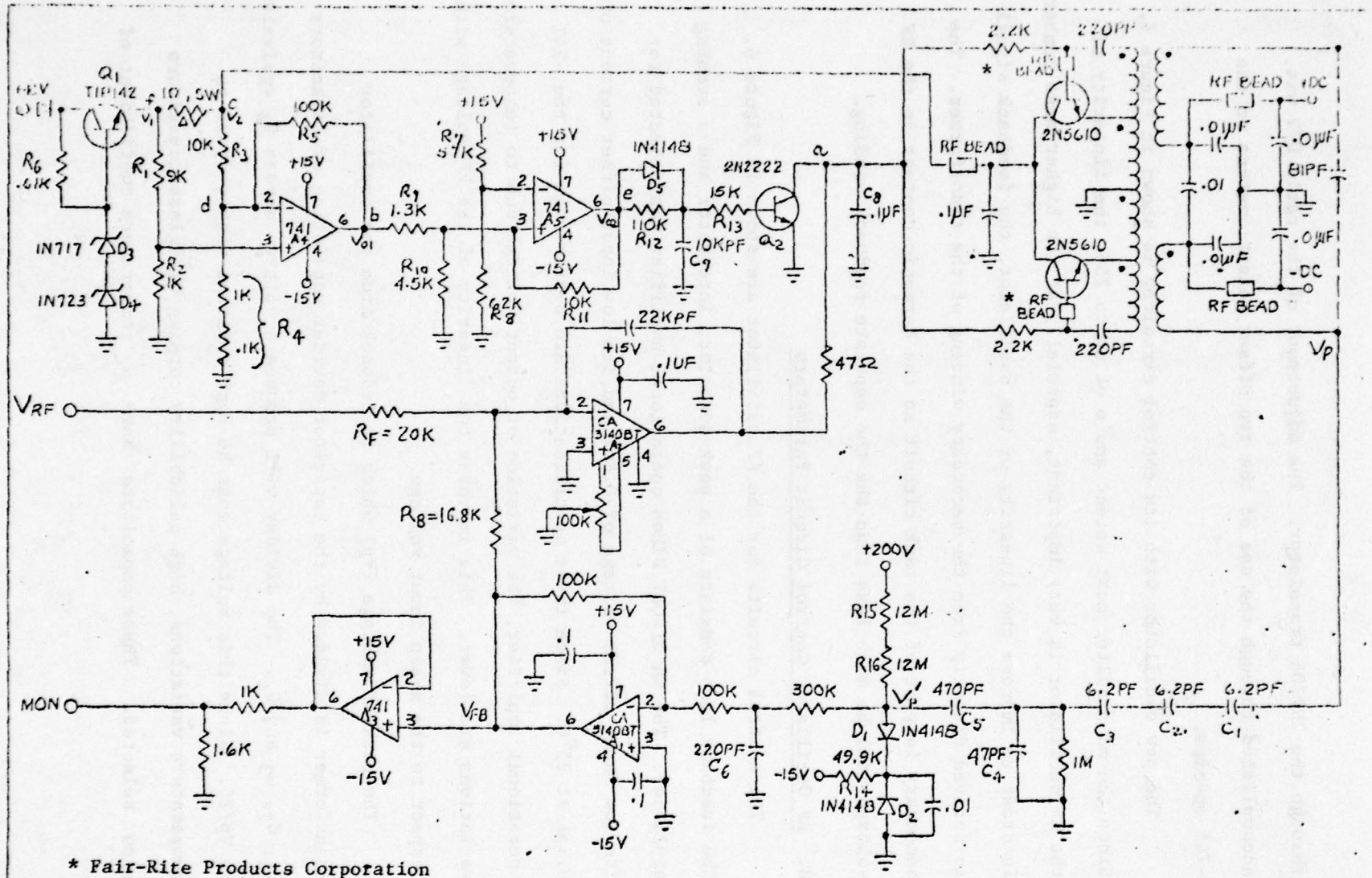

* Fair-Rite Products Corporation
No. 2673000801

FIGURE 6

TOLERANCE UNLESS OTHERWISE NOTED: DECIMALS ± .01, .005; FRACTIONALS ± 1/64; ANGULAR ± 0° 30'; SURFACE FINISH 125	DRAWN R.S. CYECHI	APPROVED FALASEK	DATE 5-30-78
	CHECKED		
	SCALE	RF OSCILLATOR	
NEXT ASSY / PROJECT / APPLICATION	MATERIAL		

NORTHEASTERN UNIVERSITY
ELECTRONIC RESEARCH LAB
COLLEGE OF ENGINEERING
BOSTON, MASS 02115

$+140 \pm 25 ppm/^{o}C$ and they will track and retrace each other to within 5ppm.

Capacitor C_5 and D_1 invert and double the voltage Vp/25. Therefore, the voltage across C_6 will be the average value of this doubled voltage. Since the gain of amplifier A_1 is 1/4, we obtain the expression for its output voltage V_{FB},

$$V_{FB} = \frac{V_p}{100\sqrt{2}} \quad . \tag{10}$$

The DC voltage U and the sweep input voltage V_{RF} are supplied from the sweep amplifier. The ratio of these two voltages is constant

$$\frac{U}{V_{RF}} = 20 \quad . \tag{11}$$

Since no current can flow into the inverting input of amplifier A_2, the currents summed at that node are;

$$\frac{V_{RF}}{R_F} = \frac{V_{FB}}{R_B} \quad . \tag{12}$$

Therefore,

$$\frac{V_{RF}}{V_{FB}} = \frac{R_F}{R_B} = \frac{U(100)\sqrt{2}}{20Vp} = \frac{U}{V} \ (5) \tag{13}$$

where, $V = \frac{V_p}{\sqrt{2}}$ (14)

so,

$$\frac{U}{V} = \frac{R_F}{R_B}\left[\frac{1}{5}\right] \qquad (15)$$

The ratio of U/V is specified to be not more than 0.236.

Therefore, if the value of 0.236 is chosen

$$\frac{R_F}{R_B} = 5(.236) = 1.18 \qquad (16)$$

Select R_F = 20K .

Then from (16), R_B = 16.9K .

Amplifier A_3 is a -741 operational amplifier used in the unity gain configuration. This amplifier is used to produce a monitor of the amplitude of the RF voltage. The output of A_3, which drives both the telemetry system and the meter on the control console, has a voltage swing of 0 to +5 volts.

IV RF TRANSFORMER

A. Empirical Determination of Transformer Size

The method of winding the RF transformer has been stated in Chapter II. Empirical determination of the core size was necessary because the equations for the inductance of toridal cores found in engineering handbooks did not correlate with the observed results. An equation for the inductance for a toridal core of rectangular section with a single winding was taken from the RCA Radiotron Designer's Handbook. This equation states that,

$$L = 0.01170N^2h \log_{10}\left[\frac{r_2}{r_1}\right], \text{ microhenrys} \quad (17)$$

where: r_1 is the inner radius of the winding

r_2 is the outer radius of the winding

h is the axial depth of the winding

N is the number of turns.

The acrylic cores we are using for these transformers have core dimensions of $r_1 = 0.57$ inches, $r_2 = 0.84$ inches and for the purpose of this example, $h = 0.9$ inches. Since each core contains 155 secondary turns of wire, we obtain a calculated inductance equal to,

$$L = 0.01170\ (155)^2(.9)\ \log_{10}\left[\frac{.84}{.57}\right] = 42.60\mu H.$$

From equation 18 we see that with a capacitive load of 81pF, the frequency of oscillation of this transformer should be 2.709 MHz.

$$f = \frac{1}{2\pi\sqrt{LC}} \quad (18)$$

The inductance of the transformer was measured on an impedance bridge and the inductance of each coil was found to be 46.10μH. This constitutes an 8% difference between the measured value and the calculated value. The frequency of oscillation that has been observed was 1.765MHz. This represents a 35% difference between the calculated frequency and the observed frequency. These results can be attributed to at least two factors. First, the equations do no take into consideration the interwinding capacitance. Secondly, very little is known about the electrical properties of these COMCO clear cast acrylic cores. Since the percentage of error is so large, empirical determination of the core size was necessary in order to predict the frequency of oscillation of these transformers to within 1% of their specified frequency.

In order to emperically determine the transformer size several cores were wound. These cores had identical inside and outside radii and differed only in their axial depth. The cores also contained an equal number of secondary windings of 155 turns apiece. These windings almost completely filled the entire core with one layer of wire except between the beginning and the end where space was left for approximately one ot two more turns. This space was left in order to prevent high voltage arcing.

The cores that were wound started with an axial depth of .5 inches were imcrenented in steps of 0.1 inches to a maximun height of oscillation is shown in Figure 7. This plot shows that there is a linear relationship, at least within this region, between the core size and the frequency. Therefore, using the plot we are able to choose

Figure 7. CORE HEIGHT VS FREQUENCY

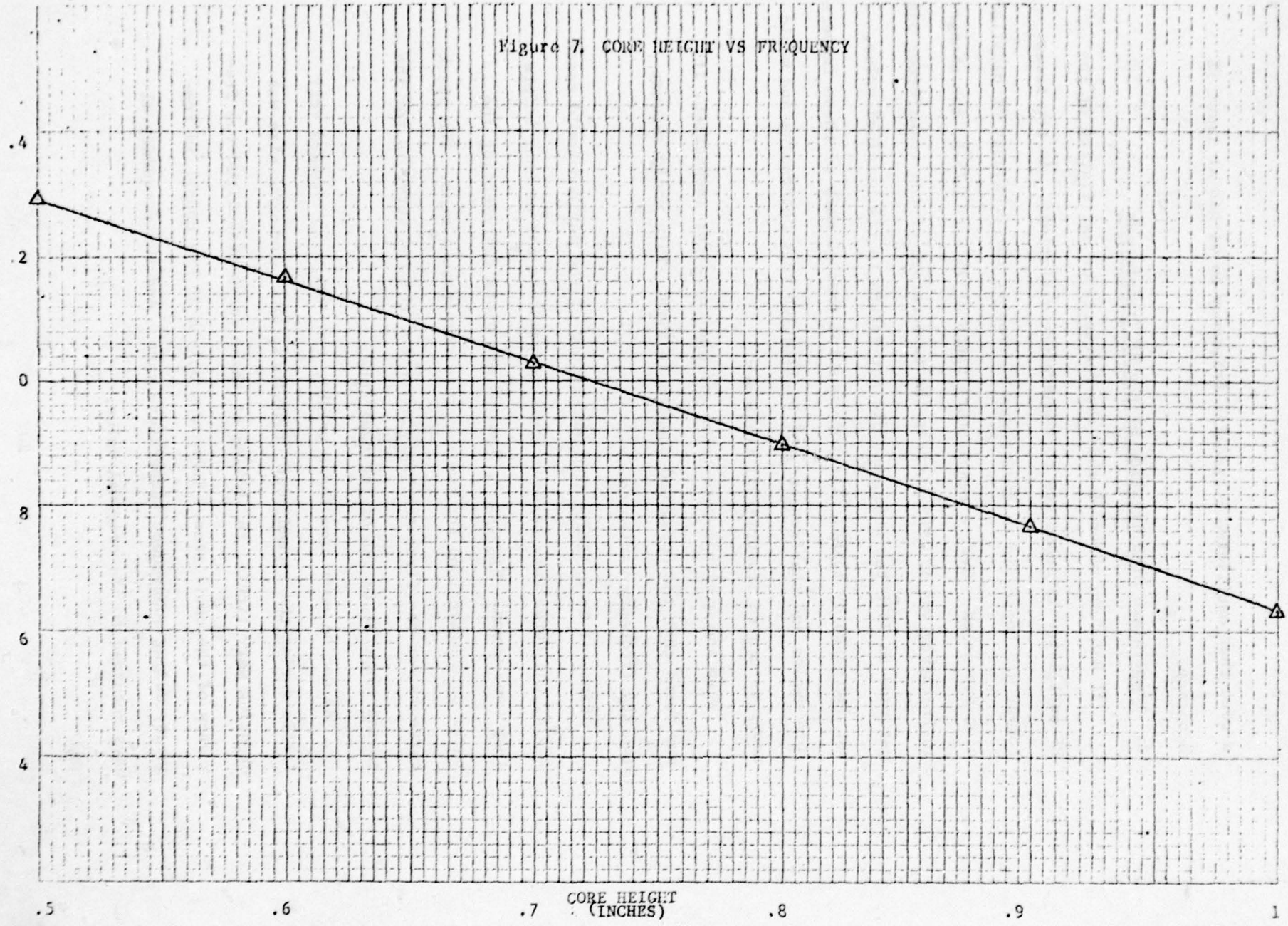

a core that oscillates a specific frequency to within at least 1% accuracy.

B. Temperature Stabilization of the RF Transformer

It has been observed that the frequency of oscillation of the RF oscillator is sensitive to temperature variations. As the transformer was heated in an environmental chamber the frequency of oscillation decreased. Over a temperature range of 75°F to 175°F, the change in frequency was 170 KHz. After the temperature of the transformer was returned to 75°F the frequency did not return to its original value, but decreased by 15KHz. The core was run through many of these temperature cycles and the frequency of oscillation kept decreasing and would never return to its original frequency.

When the windings were taken off the cores for inspection, it was found that the cores had changed in size. This would account for the frequency variation.

Since it is unlikely the temperature of the payload would reach 225°F, the cores were baked at this temperature for an hour before they were wound. Figures 8, 9 and 10 are plots representing the three core dimensions for two separate temperature runs. The black curve is for the first temperature run and the red curve is for the second temperature run of the same core.

As can be seen from these graphs, the core size changed very little during the second run. Therefore, since the core size was changing very little, the baking of these cores stabilized the frequency of the oscillator. There was only a 20 KHz change in frequency during subsequent temperature runs. And the frequency always returned to its original value.

FIGURE 8 - CORE SIZE VS TEMPERATURE

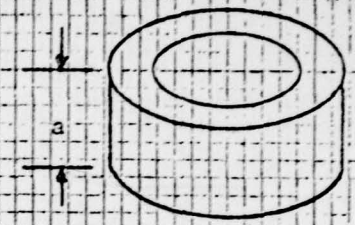

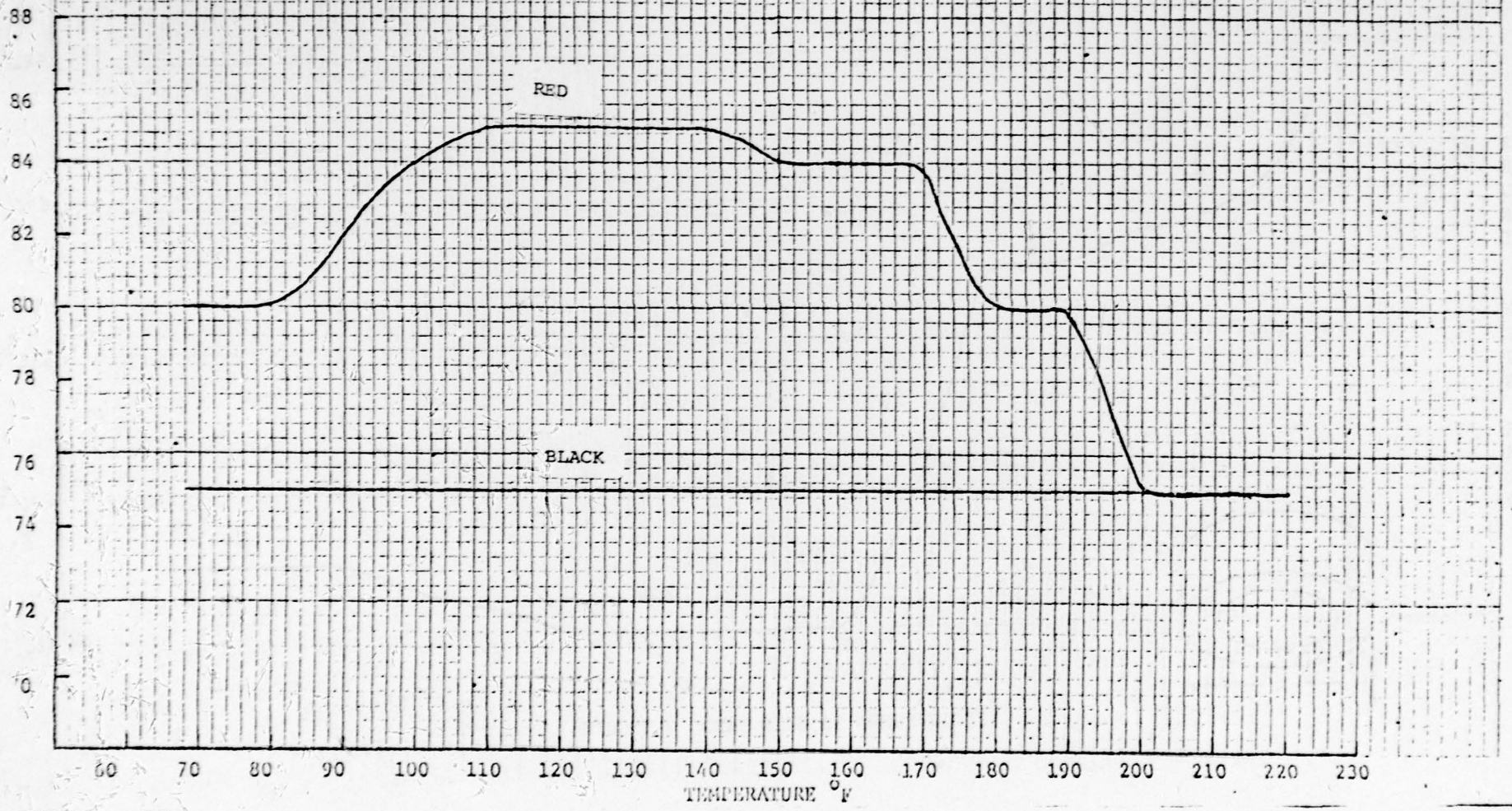

FIGURE 9 CORE SIZE VS TEMPERATURE

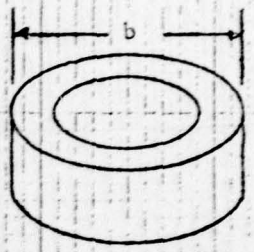

RED

BLACK

1.775
1.765
1.755
1.745
1.735
1.725

CORE SIZE INCHES

60 70 80 90 100 110 120 130 140 150 160 170 180 190 200 220 230

TEMPERATURE °F

FIGURE 10 CORE SIZE VS TEMPERATURE

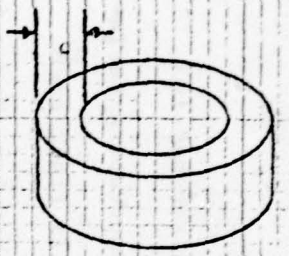

V. PEAK DETECTOR

A. Temperature Stabilization of the Peak Detector

The basic operation of the peak detector was discussed in Chapter II. This peak detector is sensitive to temperature variations. Although the capacitors C_1,C_2,C_3 and C_4 will track each other with respect to temperature variations and therefore keep the ratio of the voltages across them constant, the diode D_1 will drift approximately -2mV/^{o}C. This will cause the output of the peak detector V_{FB} to drift with temperature changes.

In order to stabilize the peak detector, diode D_2 and resistor R_{14} were added. Since the resistor R_{14} is connected to the -15 volt supply, diode D_2 has a constant current of 300μA flowing through it. When the temperature changes the voltages across the diodes D_1 and D_2 will also change. Since the cathodes of D_1 and D_2 are connected together, this change in their voltages will cancel each other and keep the voltage V_p' constant. Therefore, the peak detector output V_{FB} will remain unchanged with respect to temperature variations.

B. Linearity of the Peak Detector

At low RF voltage levels the relationship between the input voltage of the peak detector V_p and the output voltage of the peak detector V_{FB} is non-linear. This non-linearity is attributed to I-V characteristics of the diode D_1.

R_{15} and R_{16} were added to bias diode D_1. With V_p = 0 volts a current of 8.33μA will flow through D_1. As will be shown, by biasing this diode higher in its I-V curve we greatly improve the linearity of the peak detector.

The computer program on the following pages is used as an analytical aid in determining the degree of linearity of the peak detector. The main program reads from data cards the sweep input voltage and its corresponding peak RF voltage. These data points are printed and then are stored in two vectors X(I) and Y(I). From these vectors a plot is generated using Subroutine SIMPLOT.

The subroutine called LINREG will generate two important pieces of information. First an interpolating polynominal is determined. And secondly, the subroutine determines the degree of fit (coefficient of determination r^2) of these data points to the interpolating polynominal. This coefficient of determination can take on values that range from zero to one, with one being a perfect fit. In order to determine this information, the technique of linear regression by the method of least squares[4] is used. We solve for the coefficients of the linear equation

$$Y = a_1 x + a_0 \tag{19}$$

where:

$$a_1 = \frac{\Sigma xy - \frac{\Sigma x \Sigma y}{N}}{\Sigma x^2 - \frac{(\Sigma x)^2}{N}} \tag{20}$$

$$a_0 = \frac{\Sigma y}{N} - a_1 \frac{\Sigma x}{N} \tag{21}$$

N = number of data points

The coefficient of determination r^2 is defined as follows:

$$r^2 = \frac{\left[\Sigma xy - \frac{\Sigma x \Sigma y}{N}\right]^2}{\left[\Sigma x^2 - \frac{(\Sigma x)^2}{N}\right]\left[\Sigma y^2 - \frac{(\Sigma y)^2}{N}\right]} \qquad (22)$$

The program also calls Subroutine DER. This subroutine was written to determine the derivative of a group of data points. The subroutine has been generalized so it can be used if the data points are not in evenly spaced increments. Then if necessary, the derivative is interpolated for equidistant base points using subroutine SPLINE and then is plotted on a page printer plot.

Table I and Figure II are the computer outputs for the uncompensated peak detector. Table II and Figure 12 are the computer outputs for the compensated peak detector. As can be seen from the tables, the degree of fit has improved for the compensated circuit. In Figures 10 and 11 the black lines are plots of the data points while the red lines represent the linear approximations. As can be seen, the diode compensation has greatly improved the linearity of the peak detector for the low RF voltage levels.

Since the spectrum of interest begins with atomic mass units greater than or equal to ten, we see from (9) with $r_o = .273$ and a frequency of 2.3MHz that we need a peak RF voltage equal to 28.46 volts in order to sample atomic mass unit ten. As can be seen from Figure 12, this voltage lies well within the linear portion of the curve. Therefore, the improvement in the linearity of the peak detector is quite sufficient for the spectrum of interest.

```
      PROGRAM PROJECT(INPUT,OUTPUT)
      DIMENSION X(95),Y(95)
C     N=NUMBER OF DATA POINTS TO BE READ OFF DATA CARDS
      N=30
      PRINT 6
    6 FORMAT(1H1)
      PRINT 7
    7 FORMAT(13X,4HX(I),13X,4HY(I))
      READ AND PRINT DATA FROM CARDS AND STORE IN VECTORS X AND Y
      DO 1 I=1,N
      READ 2,X(I),Y(I)
    2 FORMAT(F4.2,F6.4)
      PRINT 3,X(I),Y(I)
    3 FORMAT(2(10X,F7.4))
    1 CONTINUE
C     PLOT X(I) VS Y(I)
      CALL SIMPLOT (X(1),X(N),4HX(I),10,0,X,Y(1),Y(N),4HY(I),10,0,Y,N)
      CALL LINREG(X,Y,N,A1,A0,RSQ)
      PRINT 8,A1,A0
    8 FORMAT(//10X,5HY(I)=,F7.5,2HX+F7.5)
      PRINT 9,RSQ
    9 FORMAT(//10X,41HTHE COEFFCIENT OF DETERMINATION IS R**2=F7.5)
      SW=1
      A=0.01
      CALL DER(X,Y,N,SW,A)
      STOP

      SUBROUTINE LINREG(X,Y,N,A1,A0,RSQ)
      DIMENSION X(95),Y(95)
C     INITIALIZE
      SUMX=0.
      SUMY=0.
      SUMXX=0.
      SUMXY=0.
      SUMYY=0.
C     CALCULATE SUMS
      DO 4 I=1,N
      SUMX=X(I)+SUMX
      SUMY=Y(I)+SUMY
      SUMXY=X(I)*Y(I)+SUMXY
      SUMXX=(X(I)**2)+SUMXX
    4 SUMYY=(Y(I)**2)+SUMYY
C     DETERMINE NUMERATOR AND DENOMINATOR FOR A1
C     CHANGE N TO FLOATING POINT FORMAT
      RN=N
      RNUM=SUMXY-((SUMX*SUMY)/RN)
      DEN=SUMXX-((SUMX**2)/RN)
C     DETERMINE A1 AND A0
      A1=RNUM/DEN
      A0=(SUMY/RN)-(A1*SUMX/RN)
C     DETERMINE THE COEFFICIENT OF DETERMINATION R SQUARED
      RSQ=(RNUM**2)/(DEN*(SUMYY-(SUMY**2)/RN))
      RETURN
      END
```

```
      SUBROUTINE DER(X,Y,N,SW,A)
C     SW=USERS SWITCH 1 FOR EVENLY SPACED BASE POINTS
C     0 FOR UNEVENLY SPACED BASE POINTS
C     N=NUMBER OF BASE POINTS
C     Y(I)=F(X(I))
C     A=INCREMENT FOR THE BASE POINTS
      DIMENSION X(100),Y(100),Z(100), DATA1(100,2),CURV1(100,2),DATA2(100
      2),CRUV2(100,2)
C     COMPUTE THE DERIVATIVE OF THE VECTOR Y(I)
      CALL DGT3(X,Y,Z,N,IER)
C     IF SW=0 INTERPOLATE FOR EQUIDISTANT BASE POINTS
      IF(SW)10,10,11
C     INTERPOLATE FOR EQUIDISTANT BASE POINTS
C     WE WILL INTERPOLATE FOR BOTH X AND Y AND FOR X AND Z
C     TO USE SPLINE WE MUST TRANSFER THE RESULTS INTO A 100*2 MATRIX
   10 DO 3 I=1,N
      DATA1(I,1)=X(I)
      DATA1(I,2)=Y(I)
      DATA2(I,1)=X(I)
      DATA2(I,2)=Z(I)
    3 CONTINUE
C     GENERATE BASE POINTS FOR CURV1 AND CURV2
      B=X(1)
      J=N-1
      DO 6 I=1,J
      CURV1(I,1)=B
      CURV2(I,1)=B
      B=B+A
    6 CONTINUE
      CALL SPLINE(DATA1,N,CURV1,J,0,1.,1.)
      CALL SPLINE(DATA2,N,CURV2,J,0,1.,1.)
C     PLOT CURV1 and CURV2
      DO 4 I=1,J
      X(I)=CURV1(I,1)
      Y(I)=CURV1(I,2)
    4 CONTINUE
      CALL PLOTALL(X,Y,J)
      DO 5 I=1,J
      X(I)=CURV2(I,1)
      Z(I)=CURV2(I,2)
    5 CONTINUE
      CALL PLOTALL(X,Z,J)
      GO TO 12
   11 CALL PLOTALL(X,Y,N)
      CALL PLOTALL(X,Z,N)
   12 RETURN
      END
```

X(I)	Y(I)
.0100	6.186
.0200	8.313
.0300	10.375
.0400	12.372
.0500	14.326
.0600	16.280
.0700	18.190
.0800	20.100
.0900	21.988
.1000	23.877
.1100	25.722
.1200	27.589
.1300	29.455
.1400	31.300
.1500	33.124
.1600	34.969
.1700	36.814
.1800	38.637
.1900	40.482
.2000	42.306
.2100	44.129
.2200	45.952
.2300	47.776
.2400	49.599
.2500	51.422
.2600	53.246
.2700	55.047
.2800	56.849
.2900	58.672
.3000	60.474

Y(I) = 185.755X+5.06088

THE COEFFCIENT OF DETERMINATION IS R**2=.99979

TABLE 1 COMPUTER OUTPUT FOR UNCOMPENSATED PEAK DETECTOR

X(I)	Y(I)
.0100	5.035
.0200	7.076
.0300	9.008
.0400	10.940
.0500	12.828
.0600	14.673
.0700	16.518
.0800	18.363
.0900	20.187
.1000	22.010
.1100	23.833
.1200	25.635
.1300	27.458
.1400	29.960
.1500	31.062
.1600	32.863
.1700	34.665
.1800	36.467
.1900	38.268
.2000	40.070
.2100	41.850
.2200	43.652
.2300	45.453
.2400	47.233
.2500	49.035
.2600	50.836
.2700	52.616
.2800	54.418
.2900	56.198
.3000	58.000

Y(I) = 181.458X+3.72490

THE COEFFCIENT OF DETERMINATION IS R**2 = .99991

TABLE 2 COMPUTER OUTPUT FOR COMPENSATED PEAK DETECTOR

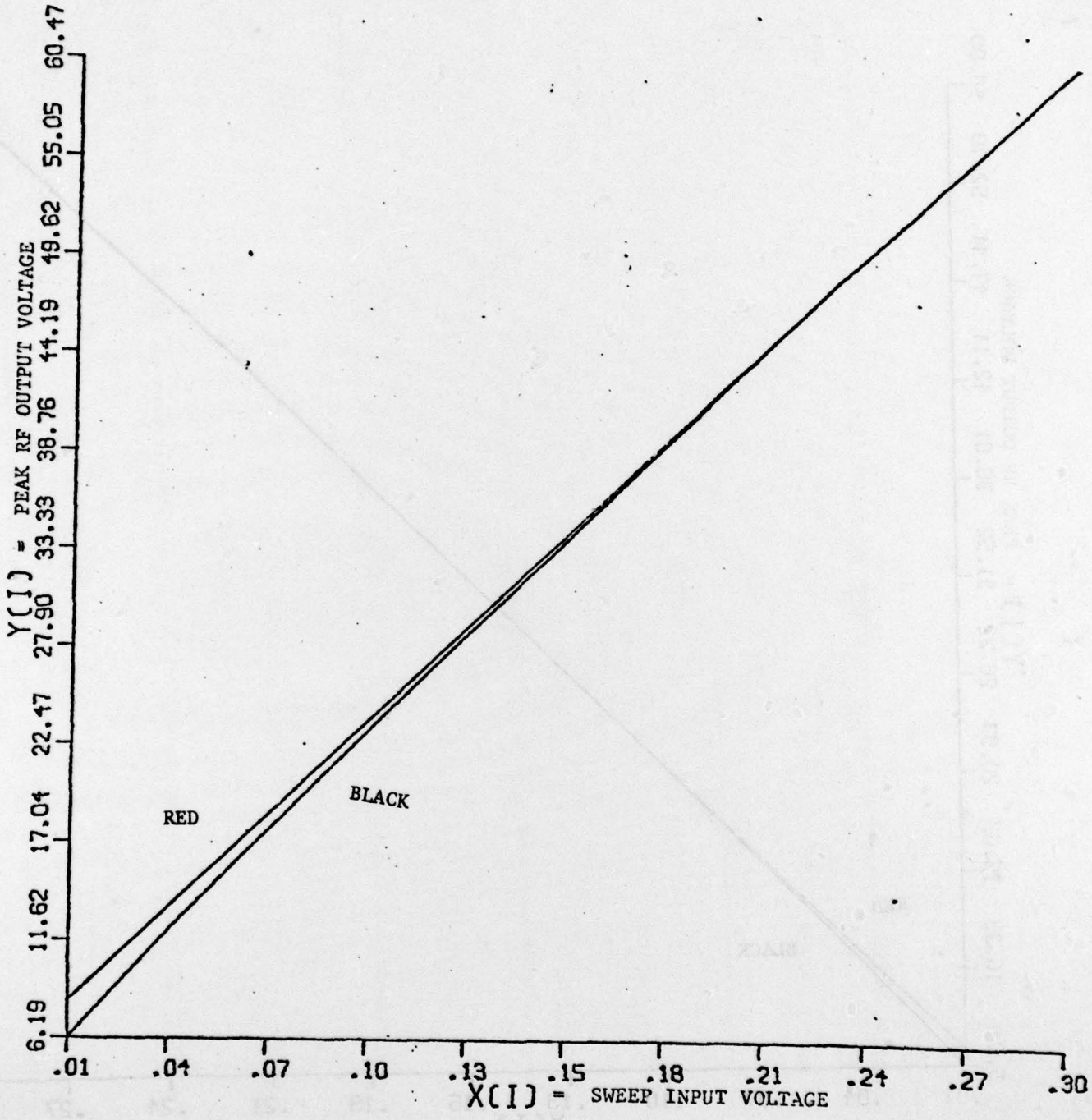

Figure 11 SWEEP INPUT VS RF OUTPUT FOR UNCOMPENSATED PEAK DETECTOR

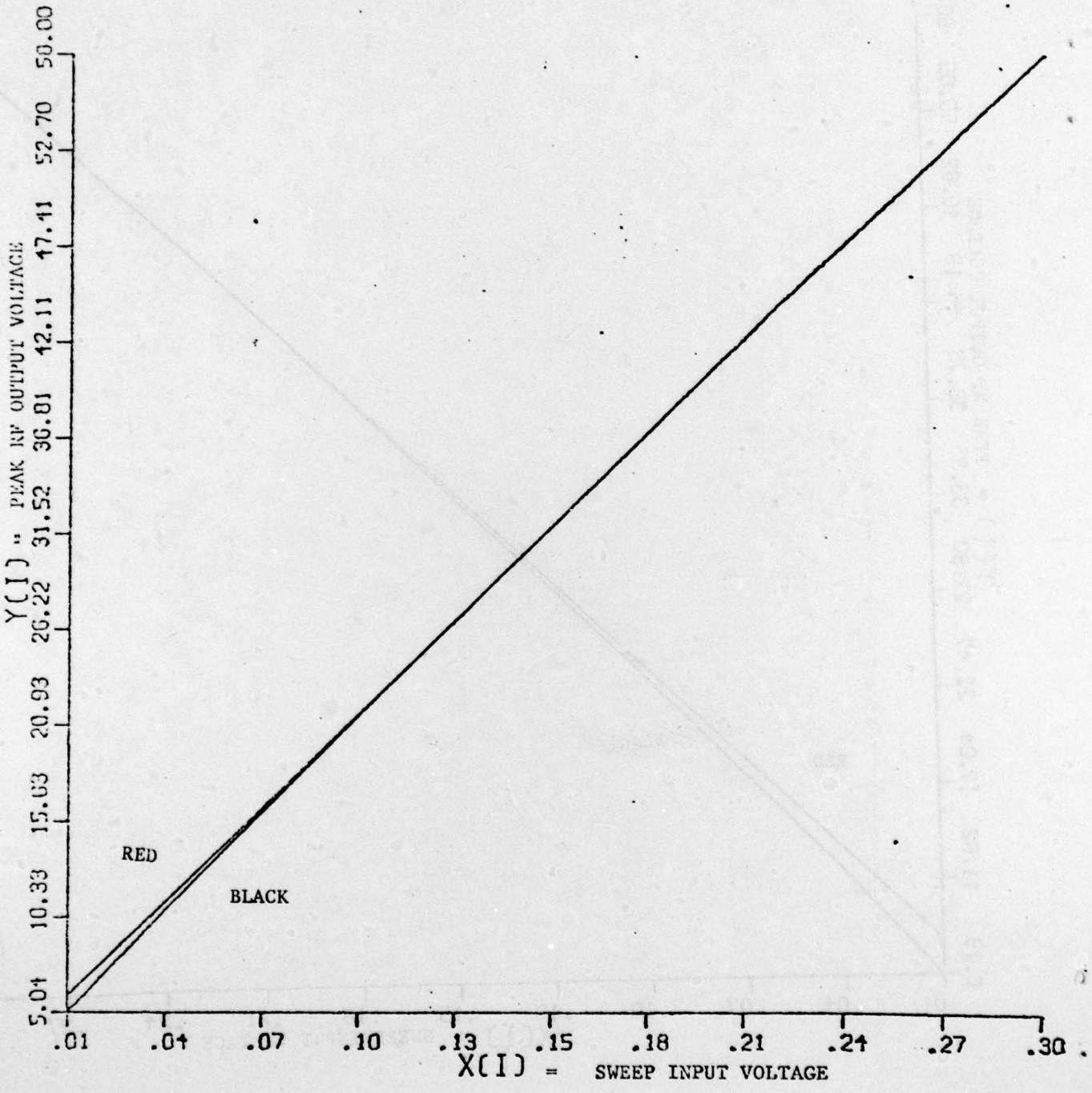

Figure 12 SWEEP INPUT VS RF OUTPUT FOR COMPENSATED PEAK DETECTOR

VI. RF OSCILLATOR PROTECTION CIRCUIT

A. Theory of Operation

The RF oscillator has an inherent problem. Transient signals or high sweep voltages may cause the oscillator to enter a "lock-up" mode of operation. In this mode the oscillator will either oscillate at a high harmonic frequency, or it will stop oscillating altogether while continuing to draw excessive current. This will cause the transistors in the oscillator to exceed their power ratings, thus destroying these devices. Also, once it enters this mode, control of the oscillator is totally lost. Only by reducing the voltage to zero and then restarting the oscillator will the normal mode of operation resume.

Conventional current limiting circuits, including foldback types, are not adequate to prevent the condition. Although the power transistors will be protected, the oscillator will not recover to the normal mode of operation. To insure proper operation of the oscillator during calibration and flight, a protection circuit has been developed.

The RF oscillator protection circuit is shown in Figure 6. The circuit consists of three sections: a voltage regulator, a current sensing and amplifier section and a Schmitt trigger. The amplifier section has been introduced in order to eliminate the possibility of accidental switching of the Schmitt trigger caused by RF radiation.

Power for the oscillator is supplied from a 40-volt battery. This 40 volts is then regulated to 36.5 volts through a series regulator which consists of the components Q_1, D_3, D_4 and R_6. The base of Q_1 is biased at 37 volts using two zenor diodes D_3 and D_4. Since the base voltage is constant, the emitter of Q_1 remains at 36.5 volts. This voltage is

then applied to the collector of the power transistors of the oscillator through a one ohm resistor.

In order to protect these transistors from exceeding their power ratings, a current of .782 amperes is a reasonable maximum value. This current will produce a difference voltage (ΔV) of .782 volts across the one ohm resistor. The ΔV is then amplified by A_4 and connected to the base of Q_2. Depending on the value of ΔV, Q_2 will either allow the sweep signal to drive the oscillator or it will force the sweep signal to approximately zero volts.

When ΔV is less than .782 volts, the output of A_5 will be at -15 volts causing Q_2 to be cutoff. This allows the sweep signal to control the oscillator. However, if ΔV reaches .782 volts, the output of A_5 will be +15 volts. This will cause Q_2 to saturate and will force the sweep signal applied to the oscillator to be the saturation voltage of the transistor which is 0.3 volts. Since the input is now 0.3 volts, ΔV will also decrease to approximately zero volts, causing the Schmitt trigger as to switch Q_2 into cutoff, thus releaseing the input.

If the sweep signal has decreased to a voltage such that ΔV will be less than .782 volts, normal operation of the oscillator will resume. However, if the sweep signal has not been decreased or has increased, the sweep input signal will again be forced to 0.3 volts by the switching of Q_2. This in turn will cause ΔV to decrease to approximately zero and the sweep signal will be released again. The protection circuit will continue to oscillate, driving the input of the RF oscillator to zero, until the sweep signal is decreased.

As described above, the power transistors of the oscillator are protected by not allowing the sweep signal to drive the oscillator above a predetermined level. This will also exclude the possibility of the oscillator entering a "lock-up" mode of operation.

B. Derivation of Circuit

The RF protection circuit uses two μA741 operational maplifiers. One is used in the basic amplifier configuration (A_4) and the other is used as a Schmitt Trigger (A_5). The output of the Schmitt trigger controls the sweep input signal by switching Q_2.

A_4 and its associated components are responsible for the detection and amplification of the voltage ΔV where $\Delta V = V1 - V_2$. Since the emitter of Q_1 is held at 36.5 volts (V_1), the voltage divider consisting of R_1 and R_2 establishes a reference voltage that is applied to the non-inverting input of A_4. The voltage divider consisting of R_3 and R_4 establishes the voltage that is applied to the inverting input of A_4. The equation for the output voltage (V_{01}) of A_4 is

$$V_{01} = -V_2 \left[\frac{R_5}{R_3 \| R_4}\right]\left[\frac{R_4}{R_3+R_4}\right] + V_1 \left[1+\frac{R_5}{R_3 \| R_4}\right]\left[\frac{R_2}{R_1+R_2}\right] \quad . \qquad (23)$$

Select the gain of A_4 to be equal to 100,

select $R_3 = 10K$,

$R_4 = 1.1K$,

$R_5 = 99K$,

(24)

then $$\frac{R_5}{R_3 \| R_4} = 100 \quad , \quad \text{and}$$

therefore:

$$V_{01} = -V_2(100)\frac{R_4}{R_3+R_4} + V_1(101)\frac{R_2}{R_1+R_2} \quad (25)$$

When $V_1 = V_2$, we want $V_{01} = 0$ volts, so

select $R_1 = 9K$,

$R_2 = 1K$ and

then $$\frac{R_4}{R_3+R_4} = \frac{101}{100}\left[\frac{R_2}{R_1+R_2}\right] \quad (.1) \quad (26)$$

With these values of components V_{01} will be zero volts for $\Delta V = 0$ and ± 10 volts for $\Delta V = 1$ volt. This voltage is then applied to the input of the Schmitt Trigger.

R_7 and R_8 establish a trigger reference voltage of 7.82 volts for the Schmitt trigger. Since A_5 is using only positive feedback, the output voltage (V_{02}) will switch between -14 volts and +14 volts depending on the voltage that is applied to the non-inverting input. The two equations for the voltage at the non-inverting input (V_L and V_H) are:

$$V_L = \left[\frac{R_{10}||R_{11}}{R_{10}||R_{11}+R_9}\right]V_{01} + \left[\frac{R_9||R_{10}}{R_9||R_{10}+R_{11}}\right][-14] \quad (27)$$

$$V_H \left[\frac{R_{10}||R_{11}}{R_{10}||R_{11}+R_9}\right]V_{01} + \left[\frac{R_9||R_{10}}{R_9||R_{10}+R_{11}}\right][+14] \quad (28)$$

A hysteresis of 2.5 volts (V_{HYS}) is incorporated into the trigger circuit,

$$V_{HYS} = V_H - V_L = 28\left[\frac{R_9||R_{10}}{R_9||R_{10}+R_{11}}\right] = 2.5 \quad (29)$$

Select $$\frac{R_9 R_{10}}{R_9+R_{10}} = 1K \quad \text{and} \tag{30}$$

therefcre: $R_{11} = 10.2K$.

Since the amplifier will switch when $V_L = 7.82$ volts, we obtain the following:

$$\frac{R_9 R_{10}}{R_9 + R_{10}} = .782R_9 \tag{31}$$

$$R_9 = \frac{1}{.782} = 1.28K \tag{32}$$

$$R_{10} = 4.57K \quad .$$

In order to reduce the average power consumption of the RF oscillator during the time that the protection circuit is oscillating, D_5, C_9, R_{12} and R_{13} have been added. This power reduction is accomplished by increasing the time during which Q_2 is in saturation. When V_{02} = +14 volts, Q_2 is saturated and C_9 will be charged. After A_5 switches, V_{02} will be -14 volts and C_9 will discharge through R_{13} and Q_2, thus increasing the time that Q_2 is in saturation. This will cause the RF oscillator to remain off for a longer period of time and therefore its average power consumption will decrease.

References

1. R. S. Narcisi (1970), Composition Studies of the Lower Ionosphere AFCRL, Office of Aerospace Research, L. G. Hanscom Field, Bedford, MA. Based on Four Lectures Presented at the International School of Atmospheric Physics, Erice, Sicily.

2. E. Arijs and D. Nevejans, A Programmable Control Unit for a Balloon Borne Quadrupole Mass Spectrometer, Belgium Institute of Space Aeronomy, Belgium.

3. R. Sukys and S. Goldberg (1974), Control Circuits for a Rocket Payload Neutralization Experiment and Other Topics, Scientific Report No. 1, AFCRL-TR-0580.

4. B. Carnahan, H. Luther and J. Wildes (1969), Applied Numerical Methods, Wiley and Sons Inc. New York.

5. P. H. Dawson, N. R. Whetton, Mass Spectroscopy Using RF Quadrupole Fields, Chap III, pp 60-185 Advances in Electronics and Electron Physics Vol 27 (1969), Academic Press NY London.

RELATED CONTRACTS AND PUBLICATIONS+

F19628-74-C-0042	1 September 1973 through 31 July 1976.
F19628-76-C-0256	1 August 1976 through 31 October 1978.
F19628-78-C-0218	18 September 1978 through present.

Sukys, R. and Goldberg, S. (1974), Control Circuits for a Rocket Payload "Neutralization and Other Topics," AFCRL-TR-74-0580.

Sukys, R., Rochefort, J.S. and Goldberg, S. (1975), "Bias and Signal Processing Circuits for a Mass Spectrometer in the Project EXCEDE: SWIR Experiment," AFGL-TR-76-200.

Rochefort, J.S. and Sukys, R. (1976), "Instrumentation Systems for Mass Spectrometers," AFGL-TR-76-200.

Rochefort, J.S. and Sukys, R. (1978), "A Digital Control Unit for a Rocket Borne Quadrupole Mass Spectrometer, AFGL-TR-78-0106.

Gerousis,V. (1979), "A Programmable Control Unit for a Balloon-Borne Mass Spectrometer Based on Intel 8085A Microprocessor," Scientific Report No. 1, AFGL-TR-

PERSONNEL

A list of the engineers who contributed to the work reported is given below:

J. Spencer Rochefort, Professor of Electrical Engineering, Department Chairman, Principal Investigator.

Raimundas Sukys, Senior Research Associate, Engineer.